

## Photovoltaic Module Modeling and Experimental Power Control using MPPT

M. Zegrar<sup>1</sup>, F.Z Zerhouni<sup>2</sup>, M.H Zerhouni<sup>3</sup>, A. Midoun

Email: <sup>1</sup> mansour.zegrar@univ-usto.dz

<sup>2</sup> fatimazohra.zerhouni@ univ-usto.dz

<sup>3</sup> mhamed.zerhouni@univ-usto.dz

<sup>1,2,3,4</sup>Electrical Engineering Faculty, Electronics Department, University of Sciences and Technology Mohamed Boudiaf of Oran USTOMB, BP 1505 El M'naouer 31000 Oran, ALGERIA



Journal of Automation  
& Systems Engineering

*Abstract-A Photovoltaic cell is a non-linear device. In this paper, the DC current-voltage (I-V) characteristics of a photovoltaic module have been modelled. Four points were used: the open-circuit voltage, the short-circuit current, and two points taken either side of the maximum power point. In this paper a method for maximizing power using DC-DC converter based on the Constant voltage Tracking (CVT) combined with the Perturb and Observe (P&O) algorithm is presented. A microcontroller is used as a support of the electronic control of converter and experimental tests are presented.*

**Keywords:** Photovoltaic generator, insulation, temperature, power, maximum power point tracking MPPT.

### 1. INTRODUCTION

NUMBER of efforts are undertaken to explore alternative energy sources in order to achieve pollution reduction. Photovoltaic (PV) energy is among renewable energies generating green electricity. Over a wide range of current and voltage, it is important to find a maximum power point (MPP) that maximizes the output power. MPP enables to extract maximum power from the PV array. In our study a simple photovoltaic model is used. The maximum power point tracker (MPPT) which is an electronic power device that significantly increases the system efficiency is realized. Constant voltage Tracking (CVT) combined with the Perturb and Observe (P&O) algorithm is adopted.

### 2. PHOTOVOLTAIC CELLS

The solar cell is a nonlinear device and can be represented as a current source model, as shown in Figure 1 [1-3].

The solar array output current is a function of insulation and temperature. The equivalent circuit of a PV cell is shown in Figure 1. The equivalent circuit of a PV cell is shown in Figure 1.

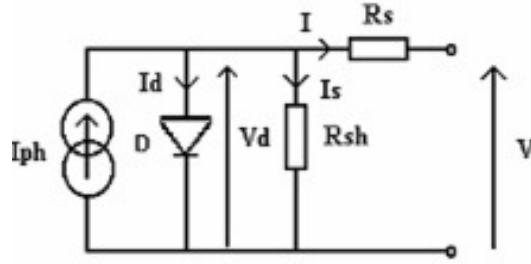


Figure 1 Equivalent circuit of a photovoltaic cell

$I_{ph} \approx I_{cc}$  : Short-circuit current.

$I_d$  : Diode current.

$R_s$ : Solar cell intrinsic series resistance whose value is usually very small.

$R_{sh}$ : Equivalent shunt resistance of the solar cell whose value is usually very large.

$I$  : Current output.

$V$  : Voltage output.

### 3. SOLAR CELLS ARRAY MODELING

In our case, a photovoltaic module is constituted of 36 solar polycrystalline cells in series (Kyocera LA 361 K51) tilted at  $35^\circ$  angle facing south. The solar cell array (SCA) is constituted of one module ( $N_s=N_p=1$ ).  $N_s$  is solar cell's number in series configuration (a branch).  $N_p$  is branch's number in parallel configuration. PV module is characterized by its current-voltage (I-V) curve. Different model of solar cells were presented in literature [4-8]. The relationship of current –voltage (I-V) for a photovoltaic module is [4]:

$$I = \left[ \left( \frac{V_{oc} - V}{V_{oc} + I_{cc} \cdot B \cdot V^2 - C \cdot V \cdot I_{cc}} \right) I_{cc} \right] \quad (1)$$

Where  $V_{oc}$  is the open-circuit voltage,  $I_{cc}$  is the short-circuit current.  $B$  and  $C$  are constants determined by:

$$B = \left[ \frac{V_{oc}}{I_{cc}} - \frac{V_2}{V_1} - \frac{(V_{oc} - V_2)}{I_1} \cdot \frac{V_2}{V_1} - \frac{V_{oc} - V_2}{I_2} \right] \cdot \frac{1}{V_1 \cdot V_2 - V_2^2} \quad (2)$$

$$C = \frac{V_{oc}}{I_{cc} \cdot V_1} + V_1 \cdot B - \frac{V_{oc} - V_1}{I_1 V_1} \quad (3)$$

Constants  $B$  and  $C$  depends on the following module parameters:

- Short circuit current  $I_{cc}$ ;
- Open circuit voltage  $V_{oc}$ ;
- Two points of coordinates ( $I_1-V_1$ ), ( $I_2-V_2$ ) taken either side of the maximum power point MPP.

Standard conditions are insulation  $E_s=1\text{kW/m}^2$ , corresponding to  $E_s= 1$  sun, and temperature  $T=25^\circ\text{C}$ .

The photovoltaic module power–voltage (P-V) is expressed as :

$$P = \left[ \left( \frac{V_{oc} - V}{V_{oc} + I_{cc} \cdot B \cdot V^2 - C \cdot V \cdot I_{cc}} \right) V \cdot I_{cc} \right] \quad (4)$$

The maximum power point (MPP) is the point on the I-V curve at which the PV module operates at maximum output power. This point corresponds to current  $I_{opt}$  and voltage  $V_{opt}$ .

Mpp voltage is determinate by:

$$V_{opt}^2 \cdot (C - B \cdot V_{oc}) - 2 \frac{V_{opt} \cdot I_{cc}}{V_{oc}} + \frac{V_{oc}^2}{I_{CC}} = 0 \tag{5}$$

Only one of the solutions obtained is considered

$$V_{opt} = \frac{\frac{2I_{cc}}{V_{oc}} - \left[ \left( \frac{2I_{cc}}{V_{oc}} \right)^2 - \frac{4V_{oc}^2}{I_{CC}} (C - B \cdot V_{oc}) \right]^{0.5}}{2 \cdot (C - B \cdot V_{oc})} \tag{6}$$

$I_{opt}$  is determined by:

$$I_{opt} = \left[ \left( \frac{V_{oc} - V_{opt}}{V_{oc} + I_{cc} \cdot B \cdot V_{opt}^2 - C \cdot V_{opt} \cdot I_{cc}} \right) I_{cc} \right] \tag{7}$$

The power-voltage P-V and current-voltage I-V curves of SCA are highly dependent on the insulation, temperature values and array configuration.

At standard conditions, ( $T=25^\circ\text{C}$ ,  $E_s=1\text{kw/m}^2$ ), the manufacturer data for one photovoltaic module are presented in Table 1:

Table 1: Photovoltaic module's data

	Manufacture's data
Voc (V)	21.2
Icc (A)	3.25
$V_{opt}$ (V)	16.9
$I_{opt}$ (A)	3.02
Rs ( $\Omega$ )	0.4

The peak power  $P_{opt}$  of the module is 51W at these conditions.

### 3.1. Insulation Effect

Figure 2 shows the I-V and P-V curves at different levels of insulation (at  $T=25^\circ\text{C}$ ) [8-9].

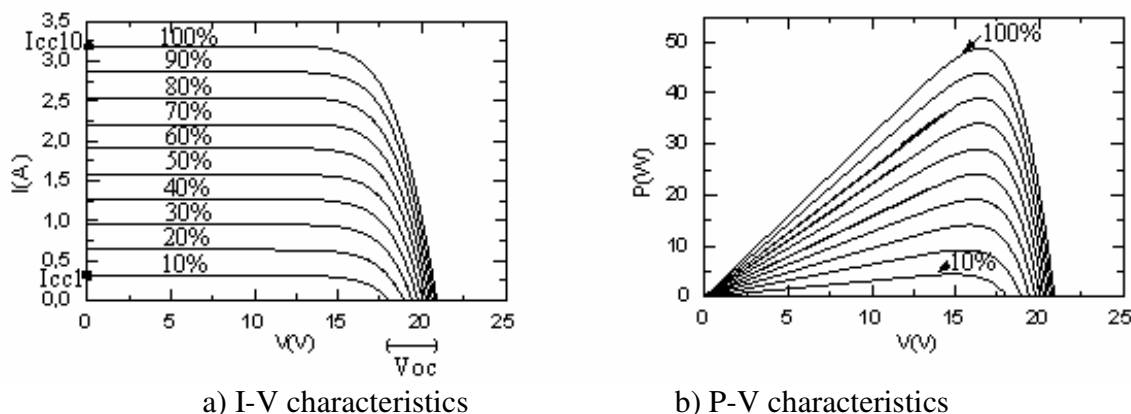
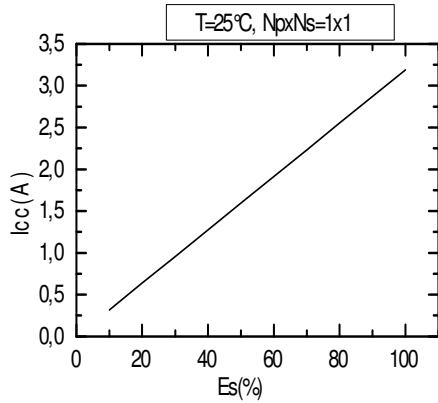
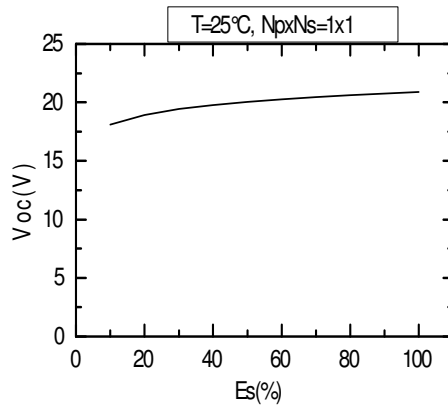


Figure 2 The SCA electrical characteristics at different levels of insulation,  $T=25^\circ\text{C}$ . When the insulation  $E_s$  increases,  $I_{cc}$  increases linearly (see Figure 3-a).  $V_{oc}$  variation versus  $E_s$  is shown in Figure 3-b. Insulation has an effect on optimal current and voltage.

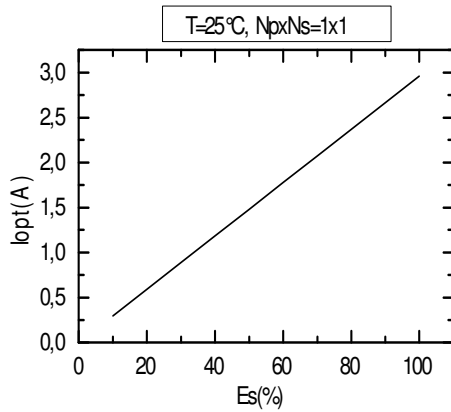
When the insulation  $E_s$  increases,  $I_{opt}$  increases slightly (see Figure 3-c).  $V_{opt}$  variation versus  $E_s$  is illustrated by Figure 3-d.  $V_{opt}$  at  $E_s=10\%$  is 15V and  $V_{opt}$  at  $E_s=100\%$  is 16.5V. When the insulation  $E_s$  increases,  $P_{opt}$  increases linearly (see Figure 3-e).  $P_{opt}=P_a=4.3W$  à 10% and  $P_{opt}=P_b=48.8W$  at  $E_s=100\%$ .



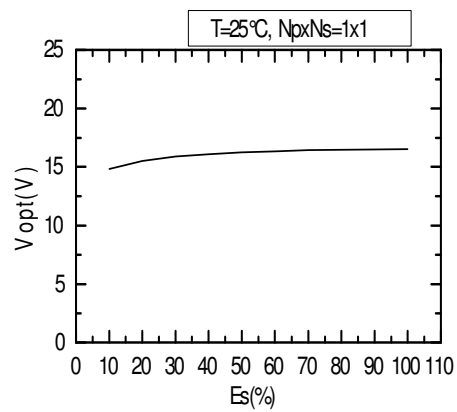
a)  $I_{cc}$  versus  $E_s$



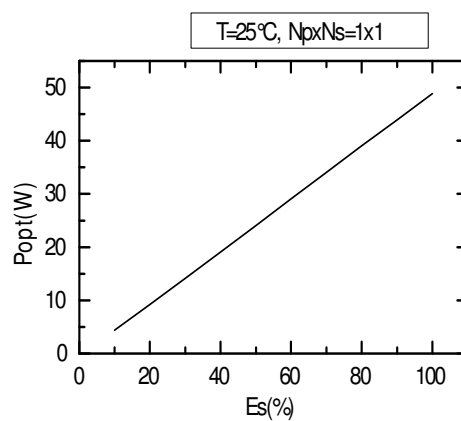
b)  $V_{oc}$  versus  $E_s$



c)  $I_{opt}$  variation versus  $E_s$



d)  $V_{opt}$  variation versus  $E_s$



e)  $P_{opt}$  Variation versus  $E_s$

Figure 3  $I_{cc}$ ,  $I_{opt}$ ,  $V_{opt}$ ,  $P_{opt}$  variations versus  $E_s$ ,  $T=25^\circ C$

### 3.2. Temperature Effect

The photovoltaic module characteristics, like any other semiconductor component is affected by temperature change. I-V and P-V obtained characteristics are shown respectively on Figure 4-a , 4-b [8-9].

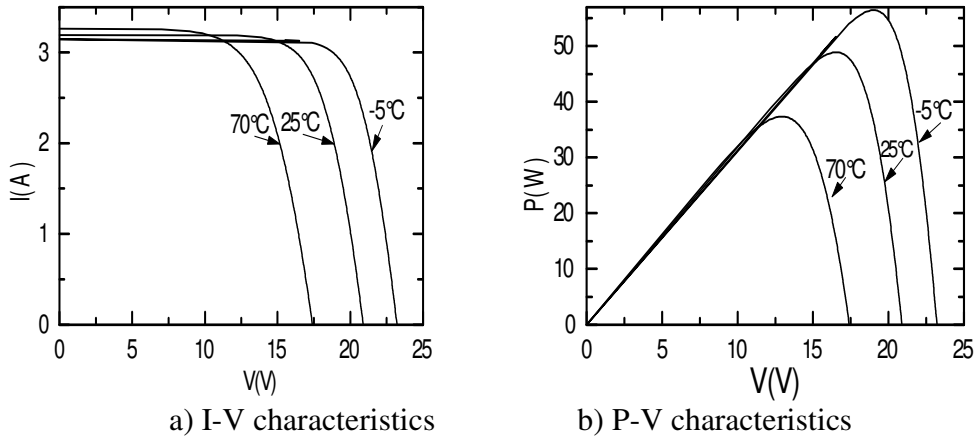


Figure 4 Effect of temperature on photovoltaic module electrical characteristics

When  $T$  increases,  $I_{cc}$  increases (Figure 5-a). The increase in temperature results also in a reduction of  $V_{oc}$  (Figure 5-b) and the available maximum power (Figure 5-c).

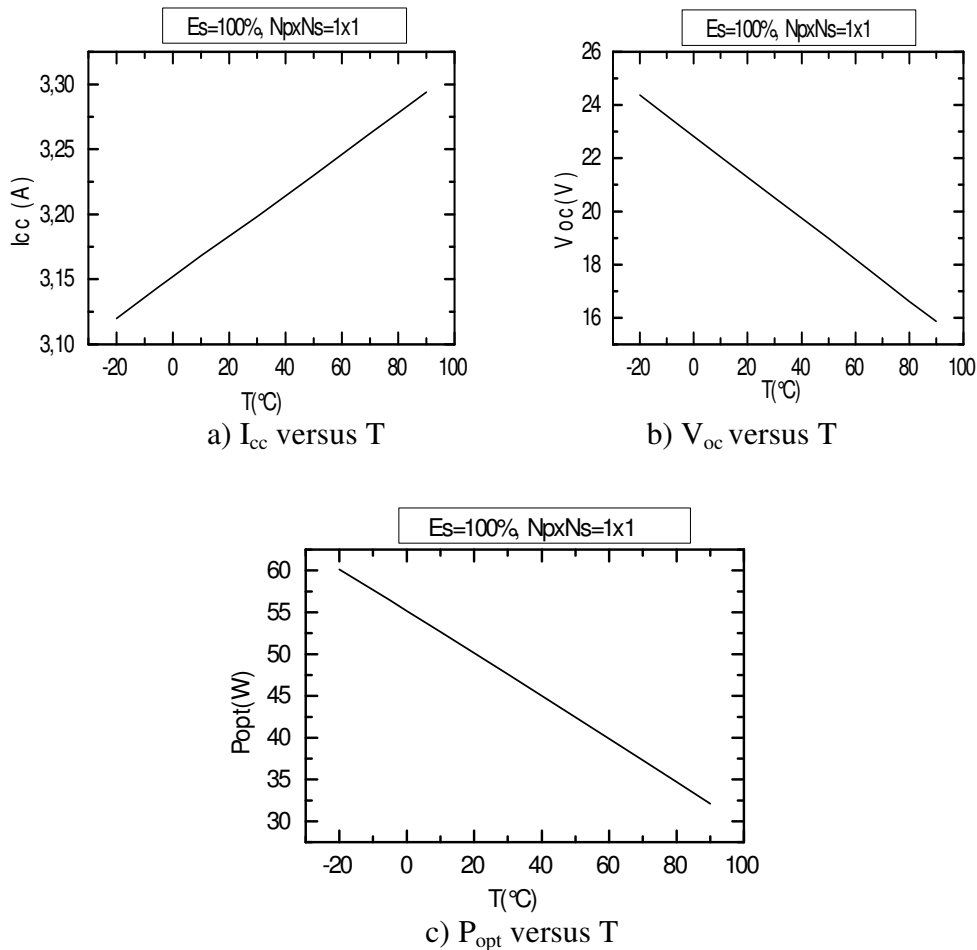


Figure 5  $I_{cc}$ ,  $V_{oc}$ ,  $P_{opt}$  variations with temperature,  $E_s=100\%$

The  $I_{cc}$  is less sensitive to temperature (Figure 5-a), this can be shown from the relation below:

$$I_{cc}(T) = I_{cc}^{st} \cdot T \cdot C_1 + C_2 \quad (8)$$

With:

$$C_1 = 4.9 \cdot 10^{-4} / ^\circ\text{C}, C_2 = 3.19\text{A},$$

T is temperature in  $^\circ\text{C}$ ,

$I_{cc}^{st}$  is short circuit current at  $T=25^\circ\text{C}$  and is equal to 3.19A.

Open-circuit voltage  $V_{oc}$  [V] is subject to temperature drift. When T increases,  $V_{oc}$  decreases (Figure 5-b). This drop is about  $77.4 \text{ mV}/^\circ\text{C}$  (Figure 5-b).  $V_{oc}$  can be approximated by:

$$V_{oc}(T) = V_{oc}^{st} \cdot [C_1 - T \cdot C_2] \quad (9)$$

With :

$V_{oc}^{st}$  : open circuit voltage at standard conditions,  $V_{oc}^{st} = 20.9\text{V}$ .

$C_1$  is a constant,  $C_1 = 1.09$ .

$C_2$  is a constant,  $C_2 = 3,7 \cdot 10^{-3} / ^\circ\text{C}$ .

T is temperature in  $^\circ\text{C}$ .

$P_{opt}$  increases when temperature decreases (Figure 5-c). The sensibility is  $0.25\text{W}/^\circ\text{C}$ .

$P_{opt}$  can be written:

$$P_{opt}(T) = P_m^{st} \cdot [C_1 + C_2 \cdot T + C_3 \cdot T^2] \quad (10)$$

$P_m^{st} = 48.9\text{W}$  is optimal power at standard conditions.

$C_1$  is constant,  $C_1 = 1.1$

$C_2$  is a constant,  $C_2 = -5.13 \cdot 10^{-3} / ^\circ\text{C}$ .

$C_3$  is a constant,  $C_3 = -1.03 \cdot 10^{-6} / (^\circ\text{C})^2$ .

The term  $CT^2$  is negligible.

From these characteristic curves, it is noted that the solar array output characteristics are nonlinear and affected by the temperature. The maximum power varies in opposite direction with the temperature (Figure 5-c).

#### 4. MAXIMUM POWER POINT TRACKER

There are several factors that mainly affect the performance of a PV system: insulation, temperature, array configuration and electric load operating condition. The Maximum power point tracker MPPT is dedicated for extracting maximum power from the photovoltaic. This power is fed to the load via the converter at varying conditions of insulation, temperature and load [8-19].

##### 4.1 The Buck-Boost Converters

There is no control over the insulation and temperature. By controlling the switching of a converter, the load conditioning can be provided. Depending on the load coupled to the photovoltaic generator, the operating voltage of SCA can be higher (point A) or lower (point B) than the optimum voltage as

shown in Figure (6). The converter interfacing the SCA to the DC bus must be able to bring back the voltage of the SCA to the maximum power point (MPP). In the case where the operating voltage is less than  $V_{opt}$  (point A), it must be increased; this can be achieved by the buck. Otherwise, the operating voltage is greater than  $V_{opt}$  (point B) and the operating current is less than the  $I_{opt}$  current. A boost converter allows the average voltage of the SCA to decrease making it possible to bring point to MPP [8-15].

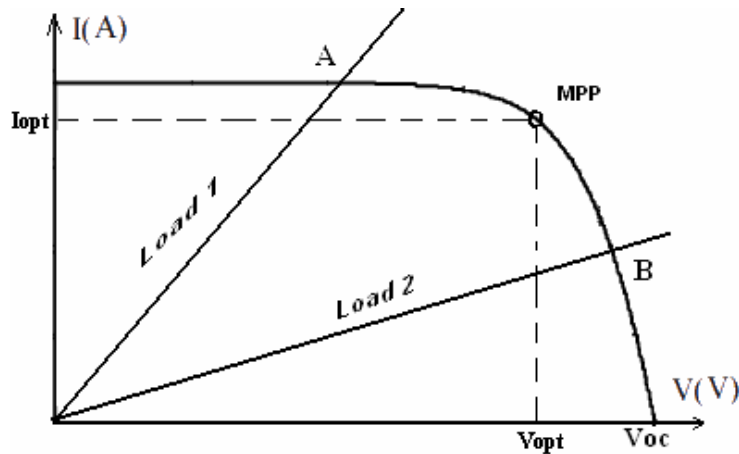


Figure 6 SCA operating point changing with load Change.

The  $V_{PV}$  input voltage and the buck-boost converter output voltage relationship is given by the following equation (11).

$$V_{out} = V_{PV} \frac{\alpha}{\alpha - 1} \quad (11)$$

The tracking of the MPP will be achieved by adjusting the duty cycle  $\alpha$ . PV panel is used to track the MPP assuming that the cells are identical and exposed to the same conditions of insulation and temperature. The tracking of the MPP is based on the measure of the current and voltage of the SCA. The result of the measurement is used to establish the treatment to track the MPP. Treatment consists in adjusting the duty cycle ( $\alpha$ ) of the buck-boost converters. Figure 7 shows the topology adopted. Outputs  $V_1$  and  $V_2$  obtained by means of a voltage divider (R1, R2) and a shunt resistor R3, are exploited through low pass filters of the type Salen & Key to evaluate the mean values corresponding respectively to the voltage and current supplied by the SCA.

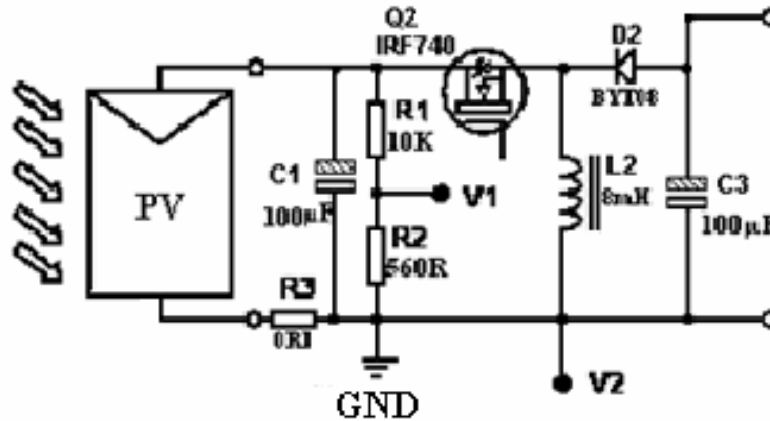


Figure 7 Experimental Buck-Boost converter electrical circuit with SCA realized at the laboratory

The voltages obtained after filtering are digitized and used to manage the organizational control of chopper working with the control signal provided by the PWM output (CCP1) of the microcontroller 16F877 via power interface.

#### 4.2 The model

Several MPPT algorithms have been developed. Many maximum power point tracking techniques for photovoltaic systems have been developed [10-15]. These techniques vary in many aspects as: simplicity, convergence, digital or analogical implementation [8-15]. The control technique mostly used consist to act on the duty cycle automatically to place the generator at its optimal value whatever the variations of insulation, temperature or sudden changes in loads which can occur at any moment. The power stage and the controller are the components of the MPPT.

The MPPT used is based on the Constant voltage Tracking (CVT) combined with the Perturb and Observe (P&O) algorithm. The Constant Voltage method uses empirical results, indicating that the voltage at MPP is around 70% to 80% of the PV open circuit voltage ( $V_{OC}$ ) for the standard atmospheric condition. The voltage corresponding to the MPP at the terminals of the module varies very little, even when the intensity of solar radiation changes [10]. The algorithm consists of two stages. First, the duty cycle is chosen such the operating point is located in the nearby MPP. This subtlety will accelerate the convergence to the MPP. Then, the (P&O) algorithm is used to tune the tracking of the MPP to get closer to finally oscillate around it as shown on the Figure 8.

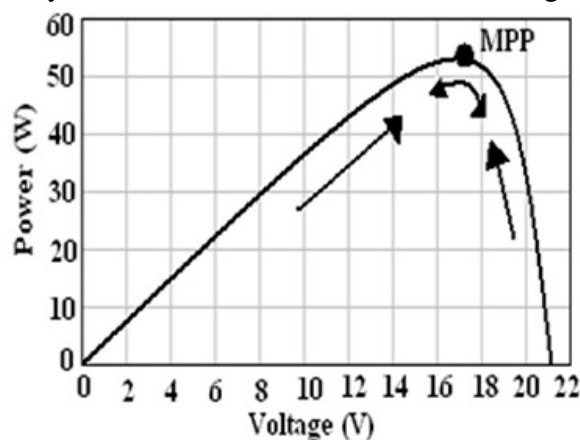


Figure 8 Graph Power versus Voltage for Perturb and Observe Algorithm.



The control technique flowchart is shown in Figure 9. Such an algorithm is implemented onto the microcontroller (16F877). The analog to digital converter peripheral is used to convert the voltages proportional to voltage and current of the SCA. The CCP1 module generates the PWM signal to control our power switch.

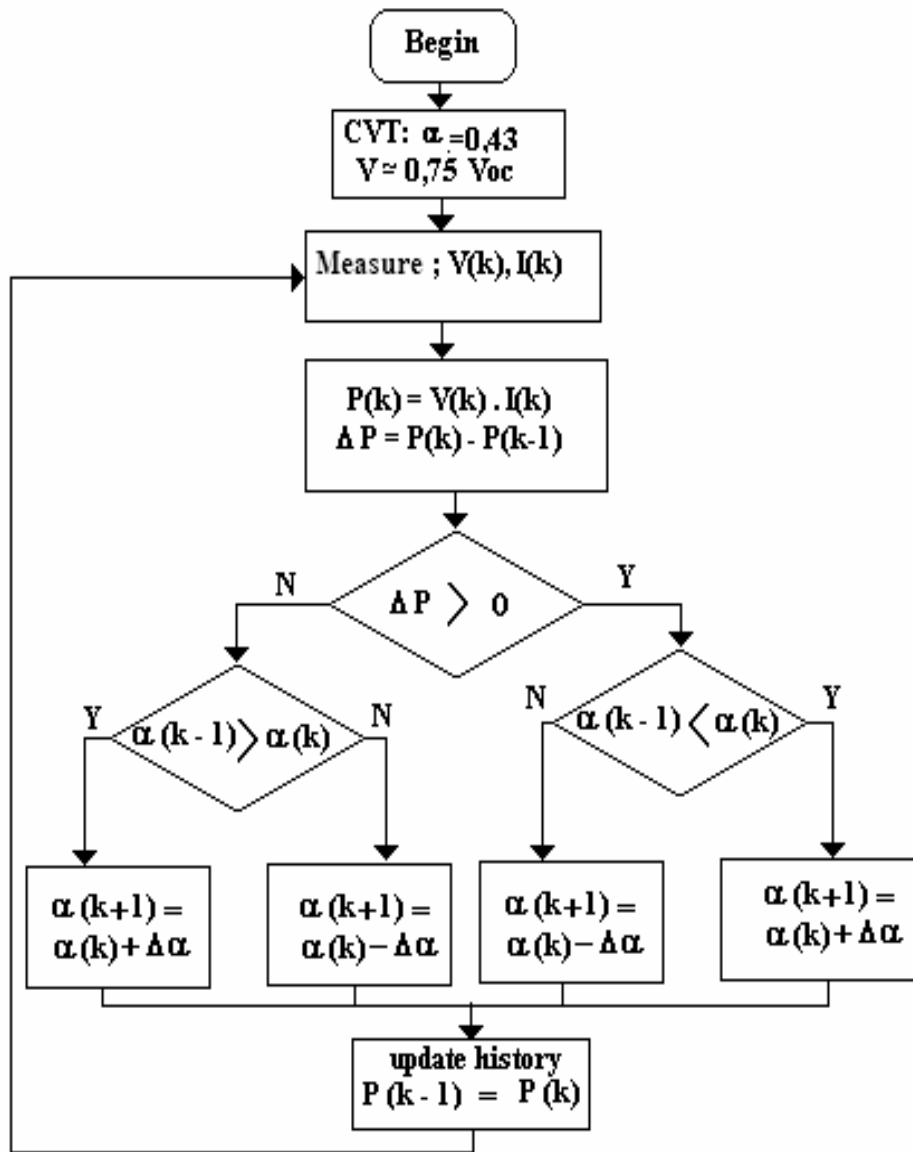


Figure 9 The P&O algorithm flowchart

In the prototype built to verify the operation of the proposed topology, control of the converter is provided by a simple microcontroller which has sufficient memory to meet the requirement of the design and thus reduce the amount of additional external parts.

## 5. EXPERIMENTAL RESULTS

This section presents the results of the experimental work using a program for the DC-DC converter. DC/DC converter is used in photovoltaic system as an interface between the photovoltaic solar cells and the load, allowing the tracking of the maximum power point (MPP) ad to force the PV module operating at MPP. The generated switching pulses are fed to the MOSFETS' gates of the prototype through an opt isolators. Some pictures of the experimental bench are given in Figure 10 and Figure 11.

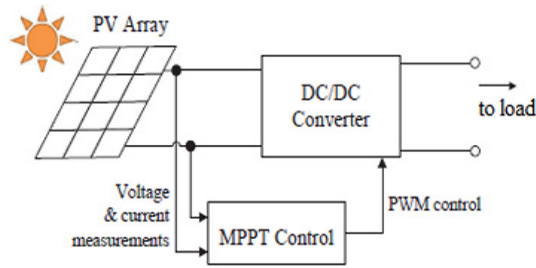
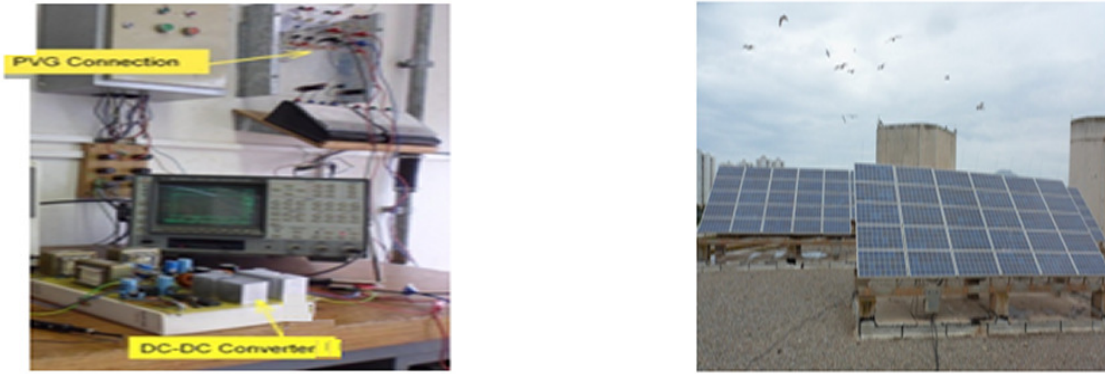


Figure 10 The schematic diagram of realization



a) Realized converter inside the Laboratory b) PV modules on the roof of the faculty

Figure 11 Photograph of the experimental bench

Figure 12 shows the measured characteristic power-voltage of one photovoltaic module.

Figure 13 shows the trajectory of the operating point using the MPPT program.

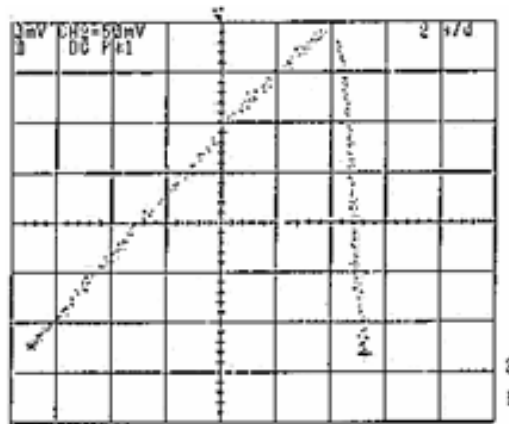


Figure 12 Experimental variation of power versus voltage of a photovoltaic module

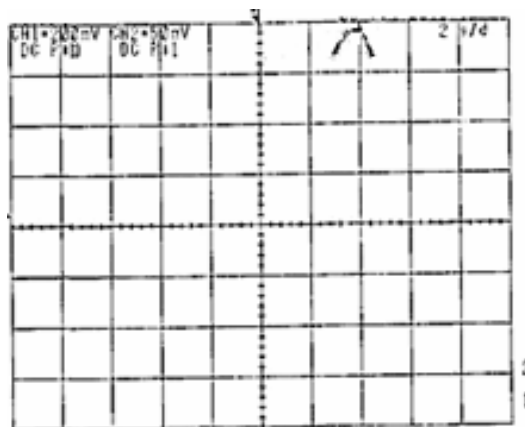


Figure 13 Experimental results obtained under MPPT control

## 6. CONCLUSION

The main aim of this work is to realize the interface of photovoltaic system to the load, the power electronics and the method to track the maximum power point (MPP) of the solar cell array. In the prototype built to verify the operation of the proposed topology, control of the converter is provided by a simple microcontroller which has sufficient memory to meet the requirement of the design and thus reduce the amount of additional external parts. The MPPT used is based on the Constant voltage Tracking (CVT) combined with the Perturb and Observe (P&O) algorithm. Practical tests have been presented. The optimal photovoltaic array output power can be extracted in real time with the proposed strategy for maximum power point tracking.

## References

- [1] F. Z. Zerhouni., M. Zegrar, M.T Benmessaoud, A.Boudghene Stambouli. A. Midoun, A, "Development of a novel strategy to improve the operation of an environmentally friendly energy system based upon photovoltaics and fuel cells, " *Journal Of Arab Universities For Basic And Applied Science*, Vol. 6, pp. 14-30, 2008.
- [2] F.Z Zerhouni, M. Zegrar, M.T Benmessaoud, A. Boudghene stambouli, "Improvement of green clean energy system's operation, " *journal of electrical system*, Vol. 5, pp. 6-26, 2009.
- [3] Yuan Li, W. Huang, H. Huang, C. Hewitt, Y. Chen, G. Fang, David L. Carroll, "Evaluation of methods to extract parameters from current–voltage characteristics of solar cells , " *Solar Energy*, Vol. 90, pp. 51–57, 2014.
- [4] M. Akbaba, "Matching three-phase AC loads to PVG for maximum power transfer using an enhanced version of the Akbaba model and double step-up converter, " *Solar energy*, Vol. 75, No. 1, pp.17-25, 2003.
- [5] A. Badoud, M.Khemliche, B. Ould Bouamama, S. Bacha, L. Fernando, L. Villa, "Bond graph modeling and optimization of photovoltaic pumping system: Simulation and experimental results, " *Simulation modelling practice and theory*, Vol. 36, pp.84-103, 2013.
- [6] G. Makrides, B. Zinsser, M. Schubert et al., "Energy yield prediction errors and uncertainties of different photovoltaic models, " *Progress in photovoltaics*, Vol. 21, No. 4, pp.500-516, 2013.
- [7] M.A. Hasan, S.K. Parida, "An overview of solar photovoltaic panel modeling based on analytical and experimental viewpoint, " *Renewable and Sustainable Energy Reviews*, Vol. 60, pp.75-83, 2016.
- [8] F.Z Zerhouni, "Développement et optimisation d'un générateur énergétique hybride propre à base de PV-PAC, " doctoral thesis, Department of Electronics, Electrical and Electronics Engineering Faculty, University of Sciences and Technology Mohamed Boudiaf ORAN energy, 2009.
- [9] F.Z Zerhouni, MH Zerhouni, M. Zegrar et al., "Proposed methods to increase the output efficiency of a photovoltaic (pv) system, " *Acta polytechnica hungarica*, Vol. 7, No. 2, pp. 55-70, 2010.
- [10] Sera, Dezso, Mathe Laszlo, Kerekes Tamas et al., " on the perturb-and-observe and incremental conductance mppt methods for pv systems, " *IEEE journal of photovoltaics*, Vol 3, No. 3, pp. 1070-1078, 2013.

- [11] Hu, Yihua, Cao, Wenping, Wu, Jiande, et al., “Thermography-Based Virtual MPPT Scheme for Improving PV Energy Efficiency Under Partial Shading Conditions, ” *IEEE Transactions on power electronics* , Vol. 29, No.(11, pp. 5667-5672, NOV 2014
- [12] Ponkarthik, N., Kalidasa Murugavel, K., “Performance enhancement of solar photovoltaic system using novel Maximum Power Point Tracking, ” *International Journal of Electrical Power and Energy Systems*, Vol. 60, pp. 1-5, 2014.
- [13] Salam Zainal, Ahmed Jubaer, Merugu Benny S., “The application of soft computing methods for mppt of pv system: a technological and status review, ” *Applied energy*, Vol. 107, pp. 135-148, 2013.
- [14] Marco Balato, Massimo Vitelli, “ A new control strategy for the optimization of Distributed MPPT in PV applications, ”*International Journal of Electrical Power & Energy Systems*, Vol. 62, pp. 763–773, 2014.
- [15] Khanna, Raghav, Zhang, Qin hao, Stanchina, William E. et al., “Maximum Power Point Tracking Using Model Reference Adaptive Control ,” *IEEE Trans. On Power Electronics*, Vol. 29, No.3, pp. 1490-1499, 2014.
- [16] S .Mohanty, B. Subudhi, P.K. Ray, “A New MPPT Design Using Grey Wolf Optimization Technique for Photovoltaic System Under Partial Shading Conditions, ”*Sustainable Energy, IEEE Transactions on*, Vol. 7, No.1, pp.181 - 188, 2016.
- [17] Yuxiang Shi, Rui Li, Yaosuo Xue, Hui Li, “High-Frequency-Link-Based Grid-Tied PV System With Small DC-Link Capacitor and Low-Frequency Ripple-Free Maximum Power Point Tracking, ”*Power Electronics, IEEE Transactions on* , Vol. 31, pp. 328 – 339, 2016.
- [18] René Aubrée, François Auger, Michel Macé, Luc Loron, “Design of an efficient small wind-energy conversion system with an adaptive sensorless MPPT strategy, ” *Renewable Energy*, Vol. 86, pp.280-291. February 2016.
- [19] Deepak Verma, Savita Nema, A.M. Shandilya, Soubhagya K. Dash, “Maximum power point tracking (MPPT) techniques: Recapitulation in solar photovoltaic systems, ” *Renewable and Sustainable Energy Reviews*, Vol. 54, pp.1018-1034, 2016.